Regional rice yield estimation based on assimilation of remote sensing data and crop growth model with Ensemble Kalman method

Jing Wang (1), Kun Yu (2), Bihui Lu (1)，Miao Tian (1)

[1] Institute of Agricultural Information, Jiangsu Academy of Agricultural Sciences, 50 Zhongling Street, Nanjing, Jiangsu Province, 210014, China

[2] Department of International Cooperation, Jiangsu Academy of Agricultural Sciences, 50 Zhongling Street, Nanjing, Jiangsu Province, 210014, China

Email: wjnj1108@sina.com; yukun108@gmail.com; 563921415@qq.com; 274587915@qq.com

KEY WORDS: Remote sensing; WOFOST; EnKF; Rice yield estimation.

ABSTRACT: Regional crop production prediction is a significant component of national food security assessment. Remote sensing has the advantage of acquiring soil surface and crop canopy radiation information, however it is hard to reveal the inherence mechanism of crop growth and yield formation. Crop growth models based on the crop photosynthesis, transpiration, respiration, nutrition are successfully applicable for yield estimation in simple point scale, however, they are hampered by the deriving of regional crop key input parameters. Data assimilation method which combines crop growth model and remotely sensed data has been proved the most potential approach in regional yield estimation. Deqing County was taken as the study area. Based on the calibration and regional of the World Food Studies (WOFOST) model, WOFOST had been used to express the characteristic of time series LAI in crop growth season. To solve the system errors of coarse resolution data extracted LAI due to the mixed pixels effect, the corrected LAI was implemented by combining the field measured LAI data and the HJ-LAI temporal trend information. Time-series LAI was assimilated through combined corrected HJ-LAI and WOFOST simulated LAI during the whole growth stage with the ensemble Kalman filter (EnKF) algorithm. The assimilated optimal LAI was used to drive the WOFOST model per-pixel to estimate the regional yield. Scheduling the assimilation of different step length observed quantities, comparing the accuracy and the efficiency of the assimilation at different time scale, we selected the proper time scale of the assimilation. The results indicate that selecting the time scale of the step length between 10 days and 16 days about the assimilation of the remote sensing information and WOFOST model is more appropriate. Compared with the statistical yield, the coefficient of determination was 0.66 and RMSE was 1.61 ton/hm. The results showed that assimilation of the remotely sensed data into crop growth model with EnKF can provide a reliable approach for estimate regional crop yield and had great potential in agricultural applications. The research can provide an important reference value for the regional crop production estimation.

1. INTRODUCTION

Rice is one of the most important crops in the world and provides staple food for more than half of the world's population (Seck et al., 2012). China produced about one third of the world's rice on about one fifth of the world's paddy rice land. Therefore, accurate regional monitoring of rice growth and yield prediction have become crucial for national food security and sustainable agricultural development in China. However, most yield-prediction methods still depend on conventional techniques, including predictions from agro-meteorological models and empirical statistical regression models between spectral vegetation indices and field-measured yields. One of the main drawbacks of such empirical regression models for estimating crop yields is that the models are only applicable for specific crop cultivars, crop growth stages, or certain geographical regions (Fang et al., 2011).

Crop growth models, based on system analysis and computer simulation techniques, can dynamically describe the fundamental processes such as photosynthesis, respiration, biomass partitioning and soil water balance. Thus, crop models have emerged as the most potent tools for yield estimation, and they have been shown to be effective for various types of crops in different countries. Several studies have confirmed that such crop models can be successfully applied to crop yield prediction at field scale (Boogaard et al., 2013; Cheng et al., 2016). However, they are also found to be limited under regional-scale extrapolation for estimating crop yield owing to uncertainties in input parameters or initial conditions (Dorigo et al., 2007). In particular, these uncertainties include two different cases: parameters that are hard to obtain at pixel or field scale and parameters that change in a single growth season or over years. Obtaining additional unknown or variational input parameters is an effective way to address these problems; however, in general, it is extremely expensive and even infeasible.

Remotely sensed data offers strong advantages over other monitoring techniques by providing a timely, synoptic, and up-to-date overview of actual crop growing conditions over large areas at multiple stages during the growing season, and the data can be utilized in conjunction with crop models to improve prediction of crop yields at a range of spatial scales (Huang et al., 2015). Furthermore, remotely sensed data can be used to complement crop model simulation results under situations that are not accounted for by the model (de Wit et al., 2012). Thus, data assimilation, an approach that incorporates field or other observations into dynamic mechanistic models, can produce more accurate estimates of model input parameters and state variables, and this approach has increasingly been used for crop growth monitoring and yield prediction, with considerable success (Ma et al., 2013; Wang et al., 2013).

With the objective to improve model performance, reinitializes crop model parameters by minimizing the differences between crop state variables simulated by the crop model and derived from remote sensing (Yan et al., 2006). Since the 1980s, when Steve Maas first attempted to combine remote sensing (RS) data for modeling (Maas, 1988), several methods for assimilating RS data into crop models have been explored. The ensemble Kalman filter (EnKF) is used in the CERES-Wheat model, WOFOST model (Li et al., 2014; Zhao et al., 2013) and SWAP (soil–water–atmosphere–plant) model (Huang et al., 2015) for many different crops.

In order to meet the remote sensing requirements of short revisit intervals and large geographical areas at regional crop yield estimation with a data assimilation model, the low spatial resolution (AVHRR, MODIS and MERIS) type instruments are widely used, which lead to a more serious heterogeneity pixel effect. Such disadvantages can be overcome by the use of high spatial resolution instruments and wide extent coverage and high revisit frequency. The small satellite constellation for environment and disaster monitoring and forecasting (HJ-1A/B) was launched by China in 2008. Two CCDs were carried by each satellite with a spatial resolution of 30 m, every 3 or 4 days the satellite could revisit the same place. HJ-1A/B provides the advantage of capturing the key spatial and temporal variations in the growing season.

In this paper, HJ-LAI data was assimilated into the WOFOST crop growth model using EnKF with the aim of predicting the yields in Deqing, Zhejiang province of China. The LAI time series profile was smoothed with Savitzky–Golay filtering algorithm first. Then, the field measured LAI was used to correct HJ-LAI data product. In order to select the proper time scale of the assimilation, we also comparing the accuracy and the efficiency of the assimilation at different time scale. The local and regional parameters were chosen to be recalibrated through a global sensitivity analysis approach. Complete details of the proposed assimilation method and analysis results are presented in the following sections.

2. MATERIALS AND METHODS

2.1 Study Area

Deqing County lies in the west of Hangjiahu Plain, with mean annual temperature ranging between 13 ℃ and 16 ℃ and annual precipitation of 1379 mm (Figure 1). The plain areas mainly distribute at the eastern Deqing, with the altitudes ranging from 4 m along the Beijing-Hangzhou Grand Canal to 721 m on the Tianmu Mountains. Deqing County is part of the single cropped rice growing region in the water network area of north Zhejiang (Xu and Wang, 2001). Deqing has a total area of 936 km^2, and the rice area in Deqing accounts for more than 91% of the major crop areas according to the statistical data of local agriculture department. The rice fields mainly concentrate in the eastern regions of Deqing with average elevation less than 20 m.

2.2 The Crop Growth Model

The WOFOST (World Food Studies) model which originates from the Center of World Food Studies located in the Netherlands was selected as a basis for our work (Doraiswamy et al., 2004), it is used for a quantitative analysis tool for the annual crop growth and yield formation process. WOFOST can simulate annual plant growth under certain weather and soil conditions, the basis of the simulation is physiological and ecological progress of crops. These progresses include light interception, CO_2 assimilation, respiration, transpiration, dry matter accumulation and distribution. The model can simulate yield estimation in two different modes, the potential mode and the water-limited mode. In the present study, the potential mode was employed.

2.3 Field Campaign Data

Field observation was conducted to obtain the important agronomic and biological parameters of rice during the entire growing season in the study area in 2013. 14 rice sample plots with areas larger than 200×200 m^2 in Deqing

County were randomly chosen in order to measure vegetation characteristics (Figure 1).The measurements mainly included plant height, LAI, above ground biomass (AGB), plant density and yield. The corresponding rice phenology dates and sample numbers for each date were recorded as well (Table 1).

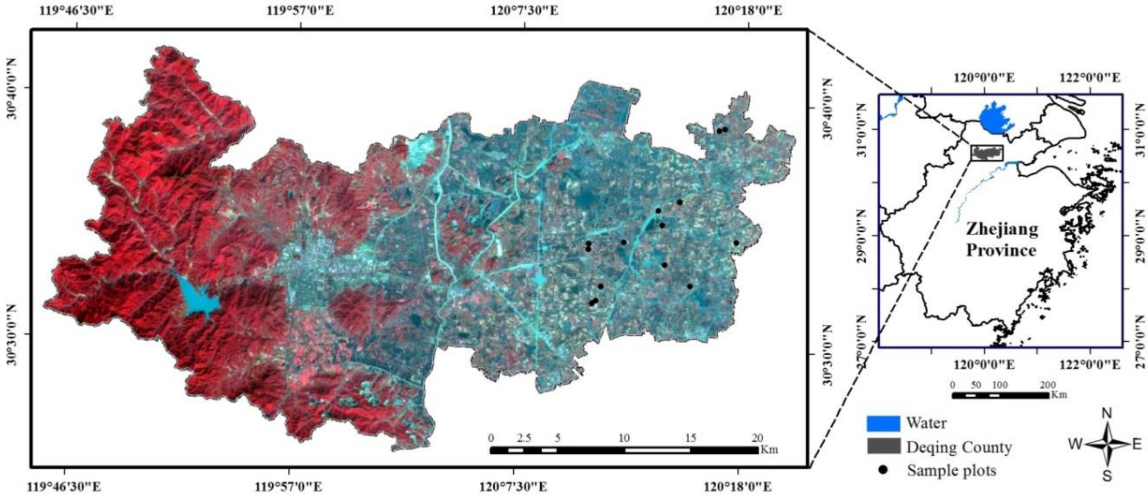

Figure 1 HJ-1A charge-coupled device (CCD) false-color composite image of the study area of Deqing County, Zhejiang Province, East China.

Table 1 Dates of the field campaigns and corresponding HJ-1A/B CCD images with sample numbers for each date.

No.	Satellite	Date	Field Campaign Date	Samples		
				LAI	AGB	Plant Density
1	HJ-1A	1 July 2013	3 July 2013	14	14	14
2	HJ-1B	18 July 2013	17 July 2013	14	14	14
3	HJ-1B	6 August 2013	6 August 2013	14	14	14
4	HJ-1A	24 August 2013	24 August 2013	14	14	14
5	HJ-1B	10 September 2013	9 September 2013 *	14	14	14
6	HJ-1B	26 September 2013	26 September 2013	14	14	14
7	HJ-1B	11 October 2013	12 October 2013	14	14	14
8	HJ-1B	26 October 2013	27 October 2013	14	14	14
9	HJ-1A	16 November 2013	15 November 2013	9	9	9

The above ground parts of rice plants were separated into leaves, stems and ear (after ear differentiation) in the lab. The leaf areas of rice were measured using a leaf area meter (LI-3000C, with conveyor belt assembly, LI-3050C; Li-Cor, Inc., Lincoln, NE, USA). All plant parts were weighted by an electronic scale in fresh condition at first. Then they were put into the oven at 105 ℃ for 30 min and kept at 70 ℃ for 72 h until reach constant weight. The dry above ground biomass was weighted with the same electronic balance and scaled to total dry AGB m^2 using plant density. The yield data was collected by harvested the rice into the laboratory. Official statistical yield data in 2013 was also collected.

2.4 Model Calibration

The WOFOST model was developed mainly for Europe. Hence, before applying the model in other geographical regions, a large set of input parameters must be calibrated for accurately simulating the entire crop growth process. Generally, the WOFOST model requires weather, soil, crop and management parameters as inputs.

Daily meteorological information was derived from Deqing weather station. These weather data provide daily estimates of daily maximum and minimum temperature, wind speed, vapor pressure and precipitation. Information regarding radiation is not available from weather stations, and therefore radiation is usually estimated at the station level using daily sunshine hour information.

Sensitive soil parameters such as saturated soil moisture content, bulk density, water content at field capacity and wilting point were collected from the local agriculture department and literatures. Other soil input parameters for the study area were derived from the 1:1,000,000 China soil database (http://www.soil.csdb.cn).

Although most of the crop parameters are genetic properties that can be decided by the crop varieties, they were determined and estimated through field measurements and were also based on the scientific works and literatures in this study area. Two important temperature accumulation related crop parameters, temperature sum from emergence to anthesis (TSUM1), and temperature sum from anthesis to maturity (TSUM2), were calculated by adding the daily average temperatures which are above 0 °C (biological zero point) from reported phenology information from agro-meteorological station of Deqing County.

In our present study, there are three main approaches used to determine input parameters in the WOFOST model according to their sensitivities. The least sensitive parameters were determined by the WOFOST defaults and related literature. The relatively stable parameters on spatial region were determined by field campaigns and the local observational station. The highly sensitive parameters with spatial variability, such as AMAXTB, SPAN and SLATB were calibrated using the FSEOPT optimization algorithm developed by Stol (Stol et al., 1992). Table 2 lists the acquired method and values of primary crop parameters in the WOFOST model.

Table 2 Main crop parameters of WOFOST model

Parameters	Description	Unit	Acquired method	Values
Phenology				
DLO	Optimum daylength for development	hr	Literature	13
TSUM1	Temperature sum from emergence to anthesis	°C·d	Meteorological data	1650
TSUM2	Temperature sum from anthesis to maturity	°C·d	Meteorological data	700
DTSMTB	Daily increase in thermal time as function of average temperature	°C·d	Literature	0-20
DVSI	Initial development stage	-	Field measured	0.10
DVSEND	Development stage at harvest	-	Custom	2
Inital				
TDWI	Initial total crop dry weight	$kg \cdot ha^{-1}$	Field measured	50
LAIEM	Leaf area index at emergence	$ha \cdot ha^{-1}$	Field measured	0.15
RGRLAI	Maximum relative increase in LAI	$ha \cdot ha^{-1} \cdot °C \cdot d$	Field measured	0.007
Green Area				
SLATB	Specific leaf area as a function of development stage	$ha \cdot kg^{-1}$	Field measured	0.001-0.0025
SSATB	Specific stem area as function of development stage	$ha \cdot kg^{-1}$	WOFOST default	-
SPAN	Life span of leaves growing at 35 ℃	d	FSEOPT	30
TBASE	Lower threshold temperature for ageing of leaves	°C	Literature	10.0
Conversion of Assimilates into Biomass				
CVL	Conversion efficiency of assimilates into leaf	$kg \cdot kg^{-1}$	Literature	0.754
CVO	Conversion efficiency of assimilates into storage organ	$kg \cdot kg^{-1}$	Literature	0.584
CVR	Conversion efficiency of assimilates into root	$kg \cdot kg^{-1}$	Literature	0.654
CVS	Conversion efficiency of assimilates into stem	$kg \cdot kg^{-1}$	Literature	0.654
Maintenance Respiration				
Q10	Relative change in respiration rate per 10 ℃	-	Literature	2
RML	Relative maintenance respiration rate leaves	$kg\ CH_2O \cdot kg^{-1}\ d$	WOFOST default	0.020
RMO	Relative maintenance respiration rate storage organs	$kg\ CH_2O \cdot kg^{-1}\ d$	WOFOST default	0.003
RMR	Relative maintenance respiration rate roots	$kg\ CH_2O \cdot kg^{-1}\ d$	WOFOST default	0.010
RMS	Relative maintenance respiration rate stems	$kg\ CH_2O \cdot kg^{-1}\ d$	WOFOST default	0.015
Partitioning				
FRTB	Fraction of total dry matter increase partitioned to roots as a function of development stage	$kg \cdot kg^{-1}$	Field measured	0-0.55
FLTB	Fraction of above ground dry matter increase partitioned to leaves as a function of development stage	$kg \cdot kg^{-1}$	Field measured	0-0.6
FSTB	Fraction of above ground dry matter increase partitioned to stems as a function of development stage	$kg \cdot kg^{-1}$	Field measured	0-0.52
FOTB	Fraction of above ground dry matter increase partitioned to storage organs as a function of development stage	$kg \cdot kg^{-1}$	Field measured	0-1

2.5 Remote Sensing Data and LAI Calculation Model

HJ-1 CCD data from June to November in 2013 over the study area were downloaded from the China Centre for Resources Satellite Data and Application (CRESDA). A total of 54 scenes of HJ-1A/B images with cloud cover less than 20% during the rice phenology in the study area were selected for the following procedures. All the images collected were all processed through radiometric calibration, atmospheric correction and geometric correction. The formula and coefficients for radiometric calibration were collected from the raw image package. The atmospheric correction was performed using the Moderate Resolution Transmission (MODTRAN) 4 model integrated in the Fast Line-of-sight Atmospheric Analysis of Spectral Hypercubes (FLAASH) module in the Environment for Visualizing Images (ENVI) package. The images were co-registered using the Second National Soil Survey Vector Map (scale 1:10,000) provided by the Deqing County Land and Resources Bureau, and the geometric accuracy was less than 0.5 pixel (15 m).

Before assimilation, time-series LAI data are required. Only cloud-free images that correspond to each field campaign date within 3 days were selected for LAI modeling. Using Savitzky-Golay (S-G) filters, daily vegetation index (VI) time-series were created from all the HJ-1 CCD images. For the entire growing season, NDVI and LAI of one crop showed a similar trend of first rising then falling, whereas the rate did not remain the same. Thus, one VI value might match two different LAI values, one from an earlier stage and the other from a later stage of the growing season. Therefore, two models were selected to simulate LAI for earlier and later stages. As the rice LAI drops after heading, in the present study, the growth stages of rice were divided into before-heading and after-heading in order to improve the estimation results. The LAI calculation model was established using a dynamic method proposed by Wang (Wang et al., 2016), before-heading LAI estimation used EVI2-BPNN (back propagation neural network) regression, and after-heading LAI estimation used NDVI-SVM (support vector machine) regression.

2.6 EnKF Asimilation Mthod

The Ensemble Kalman Filter (EnKF) is an optimal recursive data assimilation method. The EnKF performs a model forecasting where the model responses (state variables) are propagated forward in time based on the model dynamics and a filter update in which the ensemble of the model state is adjusted through incorporating available observations. Readers interested in the EnKF are referred to these studies (Evensen, 2003; Evensen, 2006) for more details.

HJ-LAI was assimilated into the WOFOST model to allow evaluation of the yield estimation accuracy. The whole process is illustrated in Figure 2.

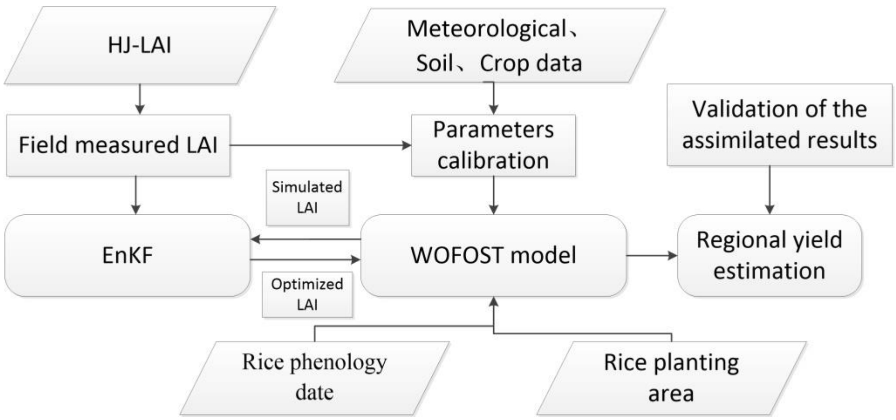

Figure 2 Flowchart of rice yield forecasting

3. RESULTS AND DISCUSSION

3.1 Influence of LAI Time Steps

Previous research indicated that time steps have great impacts on the EnKF assimilated LAI (Wit and Diepen, 2007). In the present study, we have tested different time steps of EnKF assimilation, we set different time steps of 4, 10, 16 and 20 days (scale 1 to scale 4) to analyze the effect and chose the best one to derive the final optimal results. Our testing indicated that the larger the assimilation step size, the greater the fluctuation of the LAI profile and vice versa as made clear in Figure 3-4.

When the step decreased from 4 days to 10 days (Figure 3), the assimilation time decreased from 17.4 s to 15.8 s, and the time of scale 3 and scale 4 is 15.2 s and 15.0 s, respectively. It proved that the assimilation efficiency increased to a certain extent with the increase of the assimilation time step.

Analysis from the accuracy of assimilation (Figure 4), the coincidence between LAI time series curve simulated by scale 1 and measured value was the highest, RMSE was 0.13, ARE was 3.6%. As the assimilation scale increased, the accuracy decreased significantly. When the time interval is 20 days, the RMSE reaches 0.3 and the ARE is 22.1%. The error between the final yield and the above-ground dry biomass results and measured values at the four assimilation steps also increased with time scale (Table 3). The RMSE and ARE of simulated yield and measured yield on a single point scale increased from 321 kg ha^{-1} and 3.25% at scale 1 to 1575 kg ha^{-1} and 15.96% at scale 4, respectively. The RMSE and ARE of above-ground dry biomass (TAGP) and measured values also increased from 265 kg ha^{-1} and 1.55% of scale 1 to 2698 kg ha^{-1} and 15.78% of scale 4, respectively. Scale 2 was moderate in four scales, and ARE of scale 2 was less than 10% in both LAI simulation and final yield formation. Through the above analysis, although the efficiency of assimilation scale had increased, the accuracy of assimilation had decreased. This is because after the expansion of the assimilation scale, the amount of data at the key curve turning point becomes less, and it is easy to fit during assimilated process. Under the premise of balance accuracy and efficiency, we selected the time step of scale 2 (10 days) to estimate the regional potential rice yield.

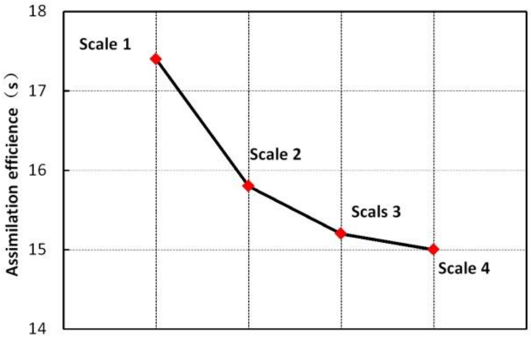

Figure 3 Assimilation efficiency at four equidistant time steps

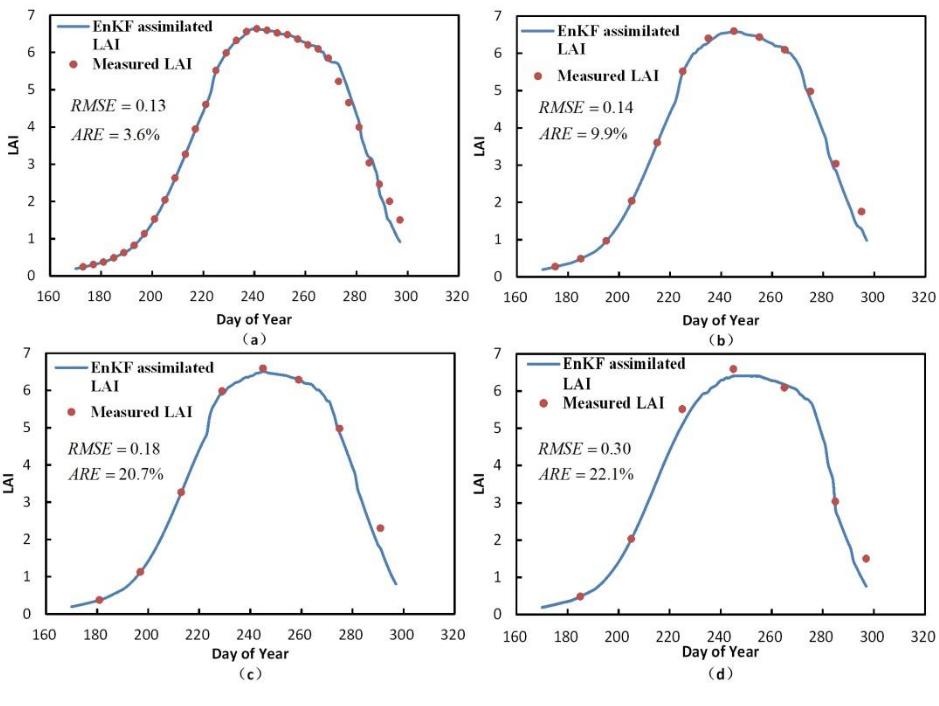

Figure 4 Assimilation accuracy of LAI at four equidistant time steps

Table 3 Assimilation result of yield (WSO) and above-ground dry biomass (TAGP) at four equidistant time steps

	Measured Yield	**Scale 1**	**Scale 2**	**Scale 3**	**Scale 4**
WSO（kg ha^{-1}）	9869	10190	10564	11401	11444
ARE（%）	-	3.25	7.04	15.52	15.96
RMSE（kg ha^{-1}）	-	321	695	1532	1575
TAGP（kg ha^{-1}）	17094	17359	17928	18952	19792
ARE（%）	-	1.55	4.88	10.87	15.78
RMSE（kg ha^{-1}）	-	265	834	1858	2698

3.2 EnKF Assimilation Yield Estimation in Potential Mode

Based on the rice area extraction results in the study area, combined with the rice transplanting period information extracted by HJ-1 CCD satellite (rice is usually transplanted within 20 days after sowing) as the initial input parameter of the WOFOST model, the rice yield estimation result of the study area was calculated pixel-by-pixel, and the output WSO value of the corresponding pixel is the corresponding yield. The estimated results were compared with the field values, as shown in Figure 5-6.

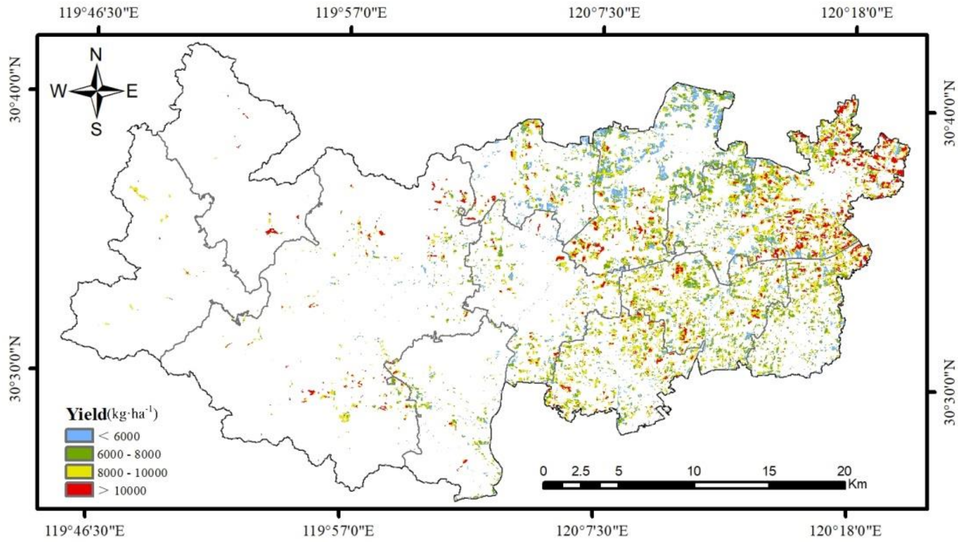

Figure 5 Predicting yield of rice in Deqing County by assimilating the WOFOST model and remote sensing

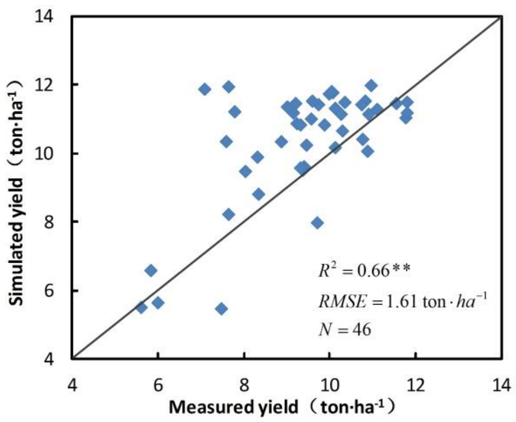

Figure 6 Correlation of rice measured yield and modeled yield after assimilation

The results showed that there was a significant correlation between the measured value and the assimilation simulation value. The R^2 of the simulated and measured values was 0.66, the RMSE was 1.61 ton ·ha^{-1}, and the average relative error ARE was 10.74%. . Overall, the yield results using remote sensing assimilation were overestimated compared to the measured values. This is because the model used a potential productivity model, which did not take the actual water and fertilizer situation into account, and did not consider the different genetic characteristics of different rice varieties, only the estimation results of the dominant varieties were considered.

In order to improve the accuracy of model estimation, more accurate input parameters are needed to improve the accuracy of area extraction and rice phenology identification. At the same time, the accuracy of assimilation state variables in time series can be further improved, and the source of model uncertainty can be reduced. In the regional distribution of rice yield, rice planting area in the western mountainous areas is small, scattered, and there are few high-yielding fields. Combined with the distribution of rice in Deqing County and the distribution map of grain production functional areas in Deqing County, high-yield fields are usually located in areas where rice fields are concentrated, or in grain production functional areas. It is proved that with the establishment and improvement of the grain production functional zone, unified management measures can make rice yield closer to potential yield.

4. CONCLUSIONS

In this study, we combined rice area mapping results, rice phenology data extraction results and remote sensing time series information results, assimilation remote sensing data and WOFOST model to estimate rice yield in the study area. Firstly, using the field measured data and FSEOPT to localize the model parameters of the main rice varieties in the study area, the parameter localization results showed that the crop model can better characterize the growth parameters of rice at a single point scale. The remote sensing information and model assimilation schemes select the Kalman filter method, and discuss the influence of different assimilation stepss on the assimilation results. Finally, under the consideration of balance assimilation efficiency and precision, the 10 days LAI remote sensing step is used to estimate the regional rice yield. The model simulation results were in good agreement with the measured results. Compared with the field measured values of the rice samples, R^2 is 0.66 and the RMSE is 1.61 ton ha^{-1}. The results show that the WOFOST model can be used for regional scale rice yield estimation, providing valuable information for accurate farming and improved cultivation management.

Acknowledgments

This work was supported by the Jiangsu Agricultural Science and Technology Innovation Fund (CX-19-3090). The authors are grateful to the anonymous reviewers who provided constructive comments and suggestions to improve this manuscript.

References

Boogaard, H., Wolf, J., Supit, I., Niemeyer, S. and van Ittersum, M., 2013. A regional implementation of WOFOST for calculating yield gaps of autumn-sown wheat across the European Union. Field Crops Research, 143(SI), pp. 130-142.

Cheng, Z., Meng, J. and Wang, Y., 2016. Improving Spring Maize Yield Estimation at Field Scale by Assimilating Time-Series HJ-1 CCD Data into the WOFOST Model Using a New Method with Fast Algorithms. Remote Sensing, 8(3034).

de Wit, A., Duveiller, G. and Defourny, P., 2012. Estimating regional winter wheat yield with WOFOST through the assimilation of green area index retrieved from MODIS observations. Agricultural and Forest Meteorology, 164, pp. 39-52.

Doraiswamy, P.C. et al., 2004. Crop condition and yield simulations using Landsat and MODIS. Remote Sensing of Environment, 92(4), pp. 548-559.

Dorigo, W.A. et al., 2007. A review on reflective remote sensing and data assimilation techniques for enhanced agroecosystem modeling. International Journal of Applied Earth Observation and Geoinformation, 9(2), pp. 165-193.

Evensen, G., 2003. The Ensemble Kalman Filter: theoretical formulation and practical implementation. Ocean Dynamics, 53(4), pp. 343-367.

Evensen, G., 2006. Data Assimilation: The Ensemble KalmanY Filter. Springer.

Fang, H., Liang, S. and Hoogenboom, G., 2011. Integration of MODIS LAI and vegetation index products with the CSM-CERES-Maize model for corn yield estimation. International Journal of Remote Sensing, 32(4), pp. 1039-1065.

Huang, J. et al., 2015. Improving winter wheat yield estimation by assimilation of the leaf area index from Landsat TM and MODIS data into the WOFOST model. Agricultural and Forest Meteorology, 204, pp. 106-121.

Huang, J. et al., 2015. Jointly Assimilating MODIS LAI and ET Products Into the SWAP Model for Winter Wheat Yield Estimation. IEEE Journal of Selected Topics in Applied Earth Observations and Remote Sensing, 8(8), pp. 4060-4071.

Li, Y. et al., 2014. Assimilating remote sensing information into a coupled hydrology-crop growth model to estimate regional maize yield in arid regions. Ecological Modelling, 291, pp. 15-27.

Ma, H. et al., 2013. Estimating regional winter wheat yield by assimilation of time series of HJ-1 CCD NDVI into WOFOST-ACRM model with Ensemble Kalman Filter. Mathematical and Computer Modelling, 58(3-4), pp. 753-764.

Maas, S.J., 1988. Using satellite data to improve model estimates of crop yield. Agronomy Journal, 80(4), pp. 655-662.

Seck, P.A., Diagne, A., Mohanty, S. and Wopereis, M.C.S., 2012. Crops that feed the world 7: Rice. Food Security, 4(1), pp. 7-24.

Stol, W., Rouse, D.I., Kraalingen, D., W.G. and Klepper, O., 1992. FSEOPT a FORTRAN program for calibration and uncertainty analysis of simulation models. European Urology Supplements, 6(1992), pp. 229.

Wang, J., Huang, J., Gao, P., Wei, C. and Mansaray, L.R., 2016. Dynamic Mapping of Rice Growth Parameters

Using HJ-1 CCD Time Series Data. Remote Sensing, 8(93111).
Wang, J., Li, X., Lu, L. and Fang, F., 2013. Estimating near future regional corn yields by integrating multi-source observations into a crop growth model. European Journal of Agronomy, 49, pp. 126-140.
Wit, A.J.W.D. and Diepen, C.A.V., 2007. Crop model data assimilation with the Ensemble Kalman filter for improving regional crop yield forecasts. Agricultural & Forest Meteorology, 146(1), pp. 38-56.
Xu, H. and Wang, K., 2001. Regionalization fro Rice Yield Estimation by Remote Sensing in Zhejiang Province. Pedosphere, 11(2), pp. 175-184.
Yan, Y., Liu, Q., Liu, Q., Li, J. and Chen, L., 2006. Methodolagy of Winter Wheat Yield Prediction based on Assimilation of Remote Sensing Data with Crop Growth Model. Journal of Remote Sensing, 10(1007-4619(2006)10:5<804:JYYGSJ>2.0.TX;2-X5), pp. 804-811.
Zhao, Y., Chen, S. and Shen, S., 2013. Assimilating remote sensing information with crop model using Ensemble Kalman Filter for improving LAI monitoring and yield estimation. Ecological Modelling, 270, pp. 30-42.